NTNU

Norwegian University of
Science and Technology

System Identification with Experiments for the milliAmpere Ferry

Anders Aglen Pedersen

December 18, 2018

TTK4551 - Specialization Project, **7.5 Credits**
Department of Engineering Cybernetics
Norwegian University of Science and Technology

Supervisor: Morten Breivik
Co-supervisor: Glenn Ivan Bitar

Abstract

The findings of system identification experiments for the autonomous passenger ferry milliAmpere are presented. milliAmpere is an autonomous ferry with the purpose to be a development platform for the full scale autonomous ferry that will transfer passengers over Nidelva in Trondheim. The focus of this report is to identify a three degree of freedom (DOF) control design model that describes the motion of the ferry. By performing experiments, measurements of steady state values, transient behaviour and input force are obtained. To ensure that the exact input force is known, a bollard pull test is completed. Damping parameters are identified by using linear regression on the steady state data. Inertia parameters are identified by using a simulator based method on the transient data. The methods are first tested on data obtained by simulating a grey box model. By comparing original parameter values for the grey box model with the estimated, the methods are verified. Then the same methods are applied on data obtained by experiments on the milliAmpere ferry.

Preface

This report is written in connection with the course TTK4551 at the Department of Engineering Cybernetics, NTNU and is **weighted 7.5 credits.** This project is the last piece of many before i go on with the master thesis and has been very rewarding and educational. I would like to thank my supervisors Morten Breivik and Glenn Bitar for giving me motivation and guidance throughout this semester, your feedback has been top notch. I will also like to thank Bjørn Olav Holtung Eriksen for being available answering questions and providing me helpful tools.

Anders Aglen Pedersen
Trondheim, December 18, 2018

Contents

Abbreviations

ASV Autonomous Surface Vehicle

CG Center of Gravity

CO Center of Origin

CV Cross Validation

DOF Degree of Freedom

GNSS Global Navigation Satellite System

IMU Inertial Measurement Unit

LTI Linear Time Invariant

QP Quadratic Problem

RTK Real Time Kinematic

ROS Robot Operating System

ROT Rate of Turn

SOG Speed Over Ground

USV Unmanned Surface Vehicle

List of Tables

List of Figures

Chapter 1

Introduction

1.1 Motivation

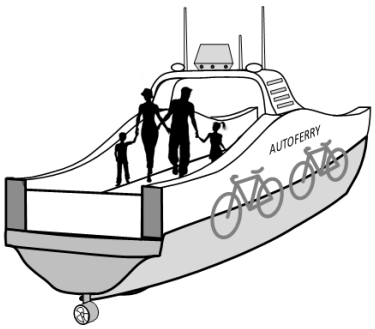

Figure 1.1: Illustration of Autoferry. https://www.ntnu.edu/autoferry

Autonomous ships are gaining interest rapidly in both research and commerce. A lot of money is being invested in this field and the global interest is increasing. KONGSBERG with Yara will be releasing the world's first fully electric and autonomous container ship, YARA Birkeland in 2020 and it is planned to be fully autonomously operational by 2022 (Kongsberg; 2018). Rolls-Royce with Finferries recently did a demonstration with a car ferry in Finland, which navigated fully autonomously on its voyage (Rolls-Royce; 2018). Across the world there are numerous cities that are built around canals, rivers etc. that needs to be crossed. A bridge is an expensive investment with high maintenance cost and also an obstacle for marine traffic. Instead by using a fully electric autonomous ferry,

flexible transportation at a lower cost and which is more environmentally friendly can be archived. At NTNu, the Autoferry project, with the vessel milliAmpere, is catching publicity in the media with its goal to make an "on demand" fully autonomous passenger ferry (Teknisk-Ukeblad; 2018). The milliAmpere is an autonomous experimental platform with the purpose to be the foundation for the development of technology for a full scale autonomous ferry that will transfer passengers safely over Nidelva in Trondheim. For further research on milliAmpere and on its way to become fully autonomous it is necessary to have a accurate mathematical description of its dynamics.

1.2 Problem Description

Accurate ship models are hard to come by, and many control approaches are dependent on rigorous descriptions of the ship dynamics. By looking at system identification techniques and ship modelling, the main objective of this project is to identify an accurate mathematical description of the milliAmpere ferry. During this project a study of different identification techniques and experiments is done and it findings will be listed in a report.

1.3 Related Work

Ship modeling is a subject that has been investigated comprehensive the last decades. In (Fossen; 2011) modelling and control of a broad variety of marine craft's that classifies at displacement vessels are covered. Maneuvering theory can be used to describe motions of marine craft in 3-DOF, that is surge, sway and yaw. It is shown how to model the hydrodynamic forces and moments, by approximating added mass and potential damping to constant values. For models which shall be used in both stationkeeping and maneuvering it is recommended to include linear potential damping and nonlinear quadratic terms. Linear damping is to ensure that the velocity converges exponentially to zero for stationkeeping, while the quadratic term is a good assumption for maneuvering models.

In (Eriksen and Breivik; 2017) a powerful approach to modeling, identification, and control of high speed autonomous surface vessels ASV's is presented. This approach suits vessels operating in displacement, semi displacement and planing

regions. The ASV used, has a propulsion system with one rear mounted engine which serves as forward propulsion and rudder. By the fact that this vessel is operating in different regions, especially semi-displacement and planing region the inertia matrix will vary with speed. Due to challenges with limitations when operating outside displacement region with the 3-DOF model as in (Fossen; 2011) a nonlinear non-first-principles model is proposed. For the identification part, a series of experiments are performed to obtain data. The experiments include tests with fixed throttle and variable rudder steps and fixed rudder with variable throttle steps. For the identification of the damping terms a polynomial function of 4th. order is used as a regressor. By using cross validation (CV) to determine regularization parameter and optimization methods such as quadratic programming (QP) the damping terms are identified by minimizing a quadratic loss function. For identification of the inertia terms, an estimate of the vessel transient response was created using local first order linear models for each transient. That is, for each step response a linear approximation of the vessel SOG was found. By simulating each transient approximation for a set of possible inertia values and selecting the inertia with smalles squared estimation error, the different inertia terms with respect to SOG was found.

A similar study by Sonneburg and Woolsey (2013) uses an unmanned surface vessel (USV) as experimental platform. This study uses a nonlinear physics based 3-DOF model with potential flow theory terms that account for the effect of added mass. By linearizing motion equations, speed and steering dynamics decouples, this reduces the complexity for the parameter identification process as it is assumed that small perturbations in sway and yaw velocity won't affect surge velocity. By expressing steering dynamics as a set of first order linear time invariant (LTI) models, with and without sideslip, it is found by experimentally testing that steering dynamics are well approximated using first order LTI models for ROT and sideslip at low speeds. At higher speeds steering motion is well described by a first order LTI model for ROT. In the identification process the steady state and transient data are split. Steady state parameters are identified using constant inputs and measuring velocities, that is yaw rate and surge velocity. By using a Savitsky-Golay filter, which uses least squares regression to fit a polynomial to signal data, dynamic parameters are identified.

1.4 Contributions

Through experimental work and identification methods a three degree of freedom (DOF) control design model for the vessel milliAmpere is provided. It is a simplified model with diagonal elements, which is considered to be sufficient to be used in controller design and in simulations. The parameters can be found in Table 3.4. Also by performing a bollard pull test, a mapping between input signals and thruster force is obtained. Experiments (Appendix A and Appendix B) are performed to gather steady state and transient velocity data. This information is used to identify model parameters using linear regression and optimization.

1.5 Outline

This report is organized in the following manner. In chapter 2, focus is on the background theory for model structures, model identification, experiments and data processing. Following in chapter 3 is results from experiments with system identification of a grey box model and the milliAmpere ferry. Finally, the conclusion is found in chapter 4.

Chapter 2

Theory

This chapter will elaborate about why a 3DOF model is suitable for this problem and by which assumptions. Then how the model is described and which model identification methods being used.

2.1 Model Structures

It exist many different methods on how to describe the motion of a ship and many aspects must be taken into account, that is, linear, nonlinear, how many DOF, external forces, operating regions, empiric procedure or first principle etc. The goal is to have a model that is accurate, not just around an operating point but for a large range of operating velocities, hence a nonlinear model is preferred. Marine craft can be classified according to their maximum operating speed (Fossen; 2011) and it is common to use the Froude number:

$$F_n := \frac{U}{\sqrt{gL}} \tag{2.1}$$

where U is vessel speed, g is gravity acceleration and L is submerged length of the vessel. The following classification can be made Faltinsen (2005)

Displacement vessels (Fn < 0.4: The boyancy force dominates relative to the hydrodynamic forces (added mass and damping)
Semi-displacement Vessel (0.4-0.5 < Fn < 1.0-1.2): The buoyanc force is not

dominant at the maximum operating speed for a high-speed submerged hull type of craft.
Planing Vessel (Fn > 1.0-1.2): The hydrodynamic force mainly carries the weight. There will be strong flow separation and the aerodynamic lift and drag forces start playing a role.

milliAmpere with its maximum speed at $2.6\frac{m}{s}$ and submerged length of $4.5m$ gives it a Froude number of 0.39. This classifies milliAmpere as a displacement vessel and this implies that the buoyancy force will be proportional to the displacement of the vessel and hydrodynamic forces consists of added mass and damping. Due to this classification it is also safe to say that inertia matrix $\boldsymbol{M}$ will be constant. When designing control systems it is beneficial to use reduced-order models since most craft do not have actuation in all DOF. For milliAmpere which will be operating at low speeds and in smooth sea states, roll, pitch and heave motion will not be dominating and is neglected for the purpose of feedback control. This implies that it will be sufficient to use a 3-DOF horizontal plane model, which includes surge, sway and yaw motion. This will also make milliAmpere fully actuated.

2.2 Kinematics & Kinetics

The kinematics and kinetics are based on the theory in (Fossen; 2011). The 3-DOF model is derived using Newton-Euler formulation and vectorial mechanics.

$$\dot{\boldsymbol{\eta}} = \boldsymbol{R}(\psi)\boldsymbol{\nu} \tag{2.2}$$

$$\boldsymbol{M}\dot{\boldsymbol{\nu}} + \boldsymbol{C}(\boldsymbol{\nu})\boldsymbol{\nu} + \boldsymbol{D}(\boldsymbol{\nu})\boldsymbol{\nu} = \boldsymbol{\tau} \tag{2.3}$$

where

$$\boldsymbol{R}(\psi) = \begin{bmatrix} \cos(\psi) & -\sin(\psi) & 0 \\ \sin(\psi) & \cos(\psi) & 0 \\ 0 & 0 & 1 \end{bmatrix} \tag{2.4}$$

and

$$\boldsymbol{\eta} = [N, E, \psi]^T$$

$$\boldsymbol{\nu} = [u, v, r]^T$$

The positions $\boldsymbol{\eta}$ are defined in North-East-Down (NED) coordinate system. The x axis points towards true north, y axis towards east and z is pointing downwards. Since milliAmpere will be navigating in a local area, an Earth fixed tangent plane on the surface is used for navigation. This is refered to as flat earth navigation (Fossen; 2011), and one can assume that this is an inertial frame, thus Newton's laws still apply. The linear and angular velocities in $\boldsymbol{\nu}$ are defined in body-fixed reference frame, with o_b in center of origin (CO). This is a moving coordinate frame that is fixed to the vessel, where x_b is in the longitudinal axis, y_b the transversal axis and z the normal axis from top to bottom.

Due to hydrodynamic forces the system will be influenced by added mass both in the inertia matrix $\boldsymbol{M}$ and in Coriolis and centripetal matrix $\boldsymbol{C}(\boldsymbol{\nu})$. And because of XZ-plane symmetry, surge is decoupled from sway and yaw. From (Fossen; 2011) it can be seen that:

$$\boldsymbol{M} = \boldsymbol{M_{RB}} + \boldsymbol{M_A}$$

$$\boldsymbol{M} = \begin{bmatrix} m - X_{\dot{u}} & 0 & 0 \\ 0 & m - Y_{\dot{v}} & mx_g - Y_{\dot{r}} \\ 0 & mx_g - Y_{\dot{r}} & I_z - N_{\dot{r}} \end{bmatrix} \tag{2.5}$$

and

$$\boldsymbol{C}(\boldsymbol{\nu}) = \boldsymbol{C_{RB}}(\boldsymbol{\nu}) + \boldsymbol{C_A}(\boldsymbol{\nu})$$

$$\boldsymbol{C}(\boldsymbol{\nu}) = \begin{bmatrix} 0 & 0 & -m(x_g r + v) + Y_{\dot{v}} v + Y_{\dot{r}} r \\ 0 & 0 & mu - X_{\dot{u}} u \\ m(x_g r + v) - Y_{\dot{v}} v - Y_{\dot{r}} r & -mu + X_{\dot{u}} u & 0 \end{bmatrix} \tag{2.6}$$

On milliAmpere, the CO is coinciding with the center of gravity (CG) and sensor measurements are transformed to (CO). This means that $x_g = 0$ in (2.5) and (2.6). When identifying the inertia parameters in (2.5) experimentally, it will be difficult to separate them from the added mass components and since experiments is based on uncoupled motion the cross terms in $\boldsymbol{M}$ is assumed zero. The values identified

on the diagonal in $\boldsymbol{M}$ will therefore contain both mass and added mass, such that

$$\boldsymbol{M} = \begin{bmatrix} m_{11} & 0 & 0 \\ 0 & m_{22} & 0 \\ 0 & 0 & m_{33} \end{bmatrix} \tag{2.7}$$

where $m_{11} = m - X_{\dot{u}}$, $m_{22} = m - Y_{\dot{v}}$ and $m_{33} = I_z - N_{\dot{r}}$. As for the $\boldsymbol{C}(\boldsymbol{\nu})$ matrix, we have

$$\boldsymbol{C}(\boldsymbol{\nu}) = \begin{bmatrix} 0 & 0 & c_{13} \\ 0 & 0 & c_{23} \\ c_{31} & c_{32} & 0 \end{bmatrix} \tag{2.8}$$

where $c_{13} = -m_{22}v$, $c_{23} = m_{11}u$, $c_{31} = -c13$ and $c_{32} = -c_{23}$.

The damping matrix $\boldsymbol{D}(\boldsymbol{\nu})$ contains both linear damping $\boldsymbol{D_l}$ and nonlinear damping $\boldsymbol{D_n}(\boldsymbol{\nu})$. The total hydrodynamic damping matrix is the sum of the linear part $\boldsymbol{D_l}$ and the nonlinear part $\boldsymbol{D_n}(\boldsymbol{\nu})$, that is

$$\boldsymbol{D}(\boldsymbol{\nu}) := \boldsymbol{D_l} + \boldsymbol{D_n}(\boldsymbol{\nu}) \tag{2.9}$$

For the vessel it is chosen to include higher order damping terms due to nonlinearities in the hydrodynamic forces. For noncoupled motion in 3 DOF the cross terms are assumed zero and the structure of the damping matrix is then diagonal. The resulting damping matrix is then:

$$\boldsymbol{D}(\boldsymbol{\nu}) = -\begin{bmatrix} X_u + X_{|u|u}|u| + X_{uuu}u^2 & 0 & 0 \\ 0 & Y_v + Y_{|v|v}|v| + Y_{vvv}v^2 & 0 \\ 0 & 0 & N_r + N_{|r|r}|r| + N_{rrr}r^2 \end{bmatrix} \tag{2.10}$$

2.3 Model Identification

In this section it is elaborated how the dynamics of the vessel is obtained through experiments and how this information is used to identify the model parameters in (2.3).

The model identification process is composed of several steps and it is convenient to divide it into:

1. Design of Experiment
2. Data collection
3. Data extraction
4. Parameter identification
5. Validation

The model consists of three matrices with unknown parameters that needs to be identified, that is $\boldsymbol{M}, \boldsymbol{C}(\boldsymbol{\nu})$ and $\boldsymbol{D}(\boldsymbol{\nu})$. The procedure is to first identify the damping parameters using a steady state approach where uncoupled motion is performed by experiments. Here it is assumed that due to uncoupled motion the Coriolis and centripetal term $\boldsymbol{C}(\boldsymbol{\nu})\boldsymbol{\nu}$ is zero, and due to steady state, velocity is constant, hence acceleration is zero. This reduces (2.3) to

$$\boldsymbol{D}(\boldsymbol{\nu})\boldsymbol{\nu} = \boldsymbol{\tau}$$

Further, inertia parameters are identified using an optimization based approach, where the loss between simulated and measured values is minimized. Last $\boldsymbol{C}(\nu)$ is identified according to (Fossen; 2011), where it is shown that $\boldsymbol{C}(\boldsymbol{\nu})$ can be represented such that it is skew-symmetric, that is

$$\boldsymbol{C}(\boldsymbol{\nu}) = -\boldsymbol{C}^T(\boldsymbol{\nu}), \forall \boldsymbol{\nu} \in \mathbb{R}^3$$

and expressed as in (2.8). This representation is proven to be useful when designing a nonlinear control system as it can be exploited by energy-based designs such as Integrator Backstepping (Fossen; 2011).

2.3.1 Design of Experiment & Test Plan

To be able to get the necessary information about the vessel to identify the parameters in (2.3), it is important to have a experiment that is well suited. As described in (Eriksen and Breivik; 2017), a similar structure for a test plan is developed for experiments on milliAmpere. The experiment will need to produce data that consists of both transient and steady state behaviour of the vessel. To be able to produce accurate parameters the data gathered must be representative of the whole operating space of the vessel. This does that a series of step responses in each DOF is constructed. The commanded input is given in percent and with a bollard pull test a mapping between percent and force is obtained.

- Steps in τ_u, $[0, 100\%]$ with increment of 20% for each step.
- Steps in τ_v, $[0, 100\%]$ with increment of 20% for each step.
- Steps in τ_r, $[0, 100\%]$ with increment of 20% for each step.

2.3.2 Data Extraction

From experimental data the measurements is collected in the set

$$\mathcal{D} = \{(\boldsymbol{\nu}_1, \boldsymbol{\nu}_2, ...\boldsymbol{\nu}_N), (\boldsymbol{\tau}_1, \boldsymbol{\tau}_2, ..., \boldsymbol{\tau}_N)\}$$

where $\boldsymbol{\nu_i} = [u_i, v_i, r_i]^T$ and $\boldsymbol{\tau_i} = [\tau_{ui}, \tau_{vi}, \tau_{ri}]^T$. Since two different methods are being used to identify damping parameters and mass parameters, it is convenient to divide it into two sets of data, that is steady state data $\mathcal{D}_s$ and transient data $\mathcal{D}_t$.

Steady State Data

From the set $\mathcal{D}$, five seconds of steady state data is extracted into

$$\mathcal{D}_s = \{(\boldsymbol{\nu}_{s1}, \boldsymbol{\nu}_{s2}, ...\boldsymbol{\nu}_{sN}), (\boldsymbol{\tau}_{s1}, \boldsymbol{\tau}_{s2}, ..., \boldsymbol{\tau}_{sN})\}$$

This set will be used when identifying the damping parameters. It can be seen that the equations of motion in steady state leaves only the damping terms and the applied force, thus (2.3) reduces to

$$\boldsymbol{D}(\boldsymbol{\nu})\boldsymbol{\nu} = \boldsymbol{\tau} \tag{2.11}$$

From this equation it is straight forward to identify the parameters with linear regression.

Transient Data

From the set $\mathcal{D}$, steady state data is extraced into

$$\mathcal{D}_t = \{(\boldsymbol{\nu}_{t\,1}, \boldsymbol{\nu}_{t\,2}, ...\boldsymbol{\nu}_{t\,N}), (\boldsymbol{\tau}_{t\,1}, \boldsymbol{\tau}_{t2}, ..., \boldsymbol{\tau}_{t\,N})\}$$

This set will be used when identifying the mass and inertia parameters. It can be seen that for uncoupled motion, (2.3) reduces to

$$\boldsymbol{M}\dot{\boldsymbol{\nu}} + \boldsymbol{D}(\boldsymbol{\nu})\boldsymbol{\nu} = \boldsymbol{\tau} \tag{2.12}$$

where the parameters in $\boldsymbol{D}(\boldsymbol{\nu})$ has been identified through steady state data analysis.

2.3.3 Linear Regression

A introduction to the relevant parts of linear regression will be provided in this section. For more details on the subject, literature such as (Hastie; 2009) is recommended.

The elements in (2.3) is assumed to have a structure that can be represented by polynomials. Linear regression is an approach used to model the relationship between a independent variable x which is denoted here as inputs and one or more dependent variables y which is denoted as outputs or responses. In general it can be formulated like this: Given a discrete data set of inputs $\{(t_1, t_2, ..., t_N), (x_1, x_2, ..., x_N)\}$, under the assumption that the output is linear in the parameters, the linear model output $\hat{Y}$ can be predicted by:

$$\hat{\boldsymbol{Y}}_{\boldsymbol{t}} = \boldsymbol{X}_{\boldsymbol{t}}^T \hat{\boldsymbol{\beta}}_{\boldsymbol{t}} + \boldsymbol{\epsilon} \tag{2.13}$$

where $\mathbf{X}$ is a row vector of inputs, $\boldsymbol{\beta}$ is the unknown parameters and $\boldsymbol{\epsilon}$ is the error term containing unmodelled dynamics, disturbances and noise. Linear regression will be used under the assumption that the output is linear in the parameters.

To fit the model to a set of training data the method of least squares can be used. In this approach the parameters β is choosen so to minimize the loss function that is the average residual sum of squares.

$$L_{ss}(\beta) = \frac{1}{N}(y_t - \boldsymbol{X_t}^T\boldsymbol{\beta})^T(y_t - \boldsymbol{X_t}^T\boldsymbol{\beta}) \tag{2.14}$$

Since this is a quadratic function of the parameters, the minimum solution always exists, but may not be unique. By differentiating $L_{ss}(\beta)$ with respect to β it can be seen that the closed form solution is:

$$\hat{\boldsymbol{\beta}} = (\boldsymbol{X}^T\boldsymbol{X})^{-1}\boldsymbol{X}^T y \tag{2.15}$$

This is a unique solution if $\boldsymbol{X}^T\boldsymbol{X}$ is nonsingular and a minimum if $\boldsymbol{X}^T\boldsymbol{X}$ is positive definite.

Regularization

In regression analysis, overfitting is a problem that makes the model correspond to closely to a set of data. The model will be very precise on predicting data points for the training set used in the regression, but will give poor predictions for a new data set. Overfitting tends to occur when the ratio between model parameters and data points are small. Regularization introduces a penalty term to the loss function with the purpose to penalize large parameter values. By introducing regularization to (2.14):

$$L_{ss}(\beta) = \frac{1}{N}(y_t - \boldsymbol{X_t}^T\boldsymbol{\beta})^T(y_t - \boldsymbol{X_t}^T\boldsymbol{\beta}) + \lambda\boldsymbol{R}(\boldsymbol{\beta}) \tag{2.16}$$

where $R(\boldsymbol{\beta}) = ||\boldsymbol{\beta}||_1$, is the $\mathcal{L}_1$ regularization, also knows as lasso. Lasso has the property of penalizing large parameter values making them go towards zero for sufficiently large values of λ (Bishop; 2006). A closed form solution that minimizes (2.16) with respect to λ does not exist, however the solution can be found by using optimization techniques such as Interior-Point methods for Nonlinear Programming (Nocedal and Wright; 2006).

Cross Validation

Cross validation (CV) is a widely used method for estimating prediction errors. It can also be used to find the value of hyper parameters. These are parameters that has to be decided before the final regression is performed. The regularization weight λ is a hyper parameter and will be determined by cross validation. The principle is to divide available data into a training set and validation set. The training set is used for parameter estimation and the validation set is used to evaluate the loss. By minimizing the loss with respect to the hyper parameter, the value of this is obtained. In sparse data sets it is recommended by Hastie (2009) to use K-Fold CV which splits the data into equal sized parts. A special case of K-fold CV is "leave one out", which evaluates all combinations of leaving one sample for the validation set.

2.3.4 Simulation Based Identification

Identifying parameters like those in $\boldsymbol{M}$ are more complicated, as parameterizing the transient response, as needed in linear regression, is not possible. To identify the inertia parameters in $\boldsymbol{M}$ a simulation based identification method is used, this is based on unpublished report by Bitar (2018). By using algorithm 1, the method can be adapted to the purpose of identifying inertia parameters on milliAmpere. It can be formulated like this: Given an experimental data set

$$\mathcal{D}_t = \{(\boldsymbol{\nu}_1, \boldsymbol{\nu}_2, ...\boldsymbol{\nu}_N), (\boldsymbol{\tau}_1, \boldsymbol{\tau}_2, ..., \boldsymbol{\tau}_N)\}$$

containing velocities and input force, which is gathered through experiments. Then a candidate model (2.12), which relates to the experimental data set, is used to simulate the velocities with the input from $\mathcal{D}_t$ and $\boldsymbol{M}$ as a parameter. A loss function is designed to be the averaged squared loss of $\boldsymbol{\nu} - \hat{\boldsymbol{\nu}}$, that is

$$\epsilon_t = \frac{1}{N}\sum_{n=1}^{N}(\boldsymbol{\nu}_n - \hat{\boldsymbol{\nu}}_n)^2 \tag{2.17}$$

where $\boldsymbol{\nu}$ are the velocities from the experimental data set and $\hat{\boldsymbol{\nu}} = \int_0^T \boldsymbol{M}^{-1}(\boldsymbol{\tau} - \boldsymbol{D}(\boldsymbol{\nu})\boldsymbol{\nu})dt + \boldsymbol{\nu}_0$, which are the velocities estimated from the candidate model. By minimizing (2.17) with respect to inertia parameters in $\boldsymbol{M}$, using Nelder-Mead

simplex algorithm as described in (Jeffrey C. Lagarias and Wright; 1998) a solution is found.

Algorithm 1 Finding parameters using simulation

procedure FIND PARAMETERS
  $t, \boldsymbol{x}, \boldsymbol{u} \leftarrow$ experimental data
  $\boldsymbol{P}_0 \leftarrow$ initial paramters guess
  $\hat{\boldsymbol{P}} \leftarrow OPTIMIZE(LossFunction(t, \boldsymbol{x}, \boldsymbol{u}, \boldsymbol{P}_0)$
  function LossFunction$(t, \boldsymbol{x}, \boldsymbol{u})$
    $\hat{x} \leftarrow SimulateCandidateModel(t, \boldsymbol{x}(t_0), \boldsymbol{u}, \hat{\boldsymbol{P}})$
    $N \leftarrow$ number of data points
    $y \leftarrow 0$
    for t_k in t **do**
      $y \leftarrow y + ||\boldsymbol{x}(t_k) - \hat{\boldsymbol{x}}(t_k)||^2$
    $y \leftarrow \frac{y}{N+1}$
    return y

Chapter 3

System Identification of milliAmpere

In this chapter the System Identication part on a grey box simulator and the vessel milliAmpere is performed. First the experiment, according to test plan in Appendix A, will be run on a grey box simulator to see if the methods described in chapter 2 is able to reproduce the actual parameters in the model used in the simulator. Finally, the experiments in Appendix A and Appendix B is performed on milliAmpere, last the results are discussed.

3.1 Grey Box Simulator

A 3-DOF model (2.3) of a vessel based on parameters in (Lyngstadaas et al.; 2018), shown in Table 3.1, is implemented in a Matlab function. The model is implemented with two thrusters placed fore and aft $0.5m$ from CO, making the thruster configuration similar to milliAmpere. The grey box model is used in a simulation to gather data used to verify our methods for parameter identification.

According to the test plan, experiments are simulated on the model, and simulation data from step responses in surge sway and yaw is gathered. The grey box model is simulated with a fourth order Runge-Kutta solver with fixed step size. To make the simulations data more realistic, random noise is added. The noise is uniformly distributed in the interval $[-0.02, 0.02]$.

Five step responses is performed in each DOF on the grey box model. Each step has an increase of 20% of 200 Newton which is defined as the maximum force for the grey box model.

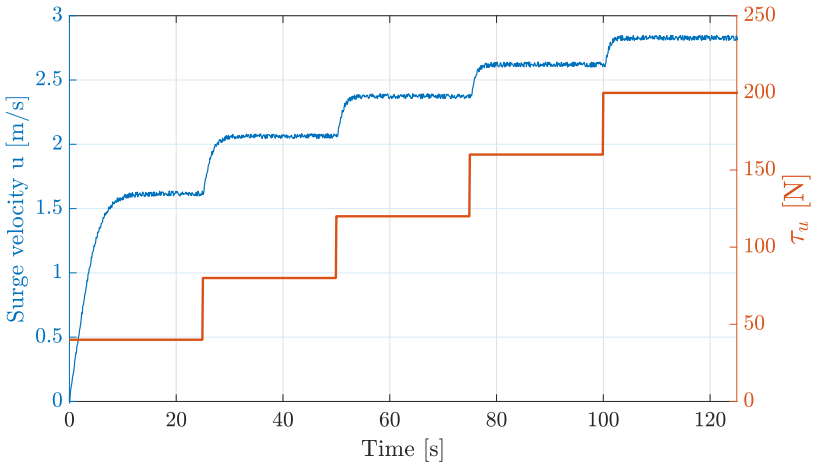

Figure 3.1: Simulation of step responses in surge. Five steps with increment of 20% each step on greybox ship model.

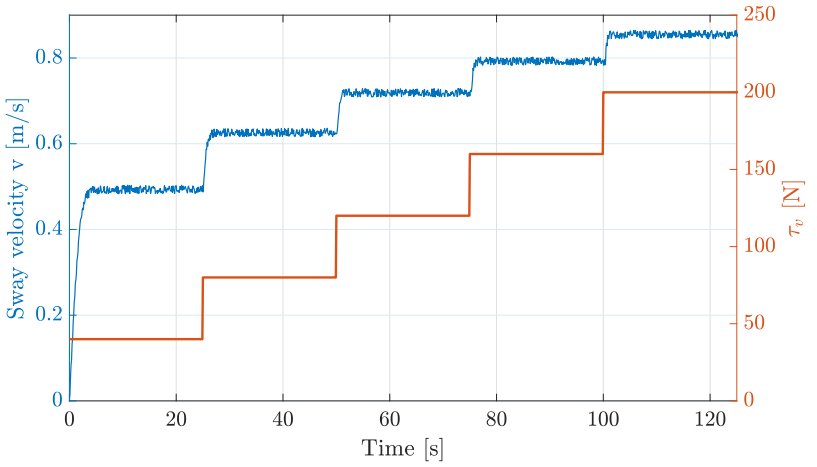

Figure 3.2: Simulation of step responses in sway. Five steps with increment of 20% each step on greybox ship model.

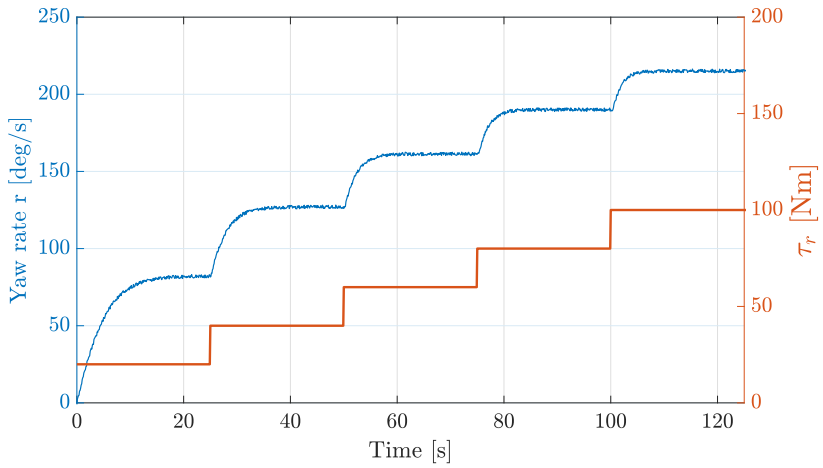

Figure 3.3: Simulation of step responses in yaw. Five steps with increment of 20% each step on greybox ship model.

3.1.1 Steady State

Figures 3.1 through 3.3 shows the input steps and the correlating step response for the simulated vessel. From these step responses five seconds of steady state values are gathered in set $\mathcal{D}_s = \{(\boldsymbol{\nu}_{s1}, \boldsymbol{\nu}_{s2}, ...\boldsymbol{\nu}_{sN}), (\boldsymbol{\tau}_1, \boldsymbol{\tau}_2, ..., \boldsymbol{\tau}_N)\}$. For the reduced (2.11) we want to identify the parameters in the damping matrix.

$$\boldsymbol{\tau} - \boldsymbol{D}(\boldsymbol{\nu})\boldsymbol{\nu} = \mathbf{0}$$

The damping matrix is substituted with $\boldsymbol{D}(\boldsymbol{\nu})\nu = \beta^T f(\boldsymbol{\nu})$, where

$$f(\boldsymbol{\nu}) = [u, v, r, |u|u, |v|v, |r|r, u^3, v^3, r^3]^T \tag{3.1}$$

$$\boldsymbol{\beta} = -[X_u, X_{|u|u}, X_{uuu}, Y_v, Y_{|v|v}, Y_{vvv}, N_r, N_{|r|r}, N_{rrr}]^T \tag{3.2}$$

The average squared loss becomes:

$$\epsilon = \frac{1}{N}\sum_{i=1}^{N}(\boldsymbol{\tau_i} - \boldsymbol{\beta}^T f_i(\boldsymbol{\nu_i}))^2 + \lambda||\boldsymbol{\beta}||_1 \tag{3.3}$$

Where λ is decided by cross validation. By minimizing (3.3) with respect to $\boldsymbol{\sigma}$ using nonlinear optimization, a solution is found.

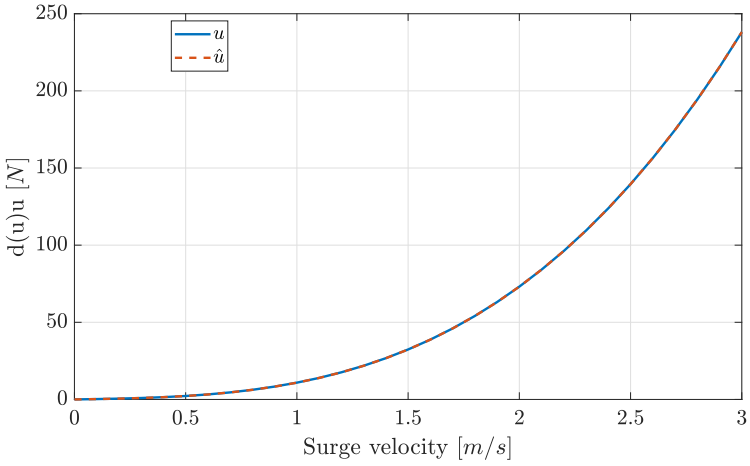

Figure 3.4: Surge damping of grey box model compared to estimated surge damping

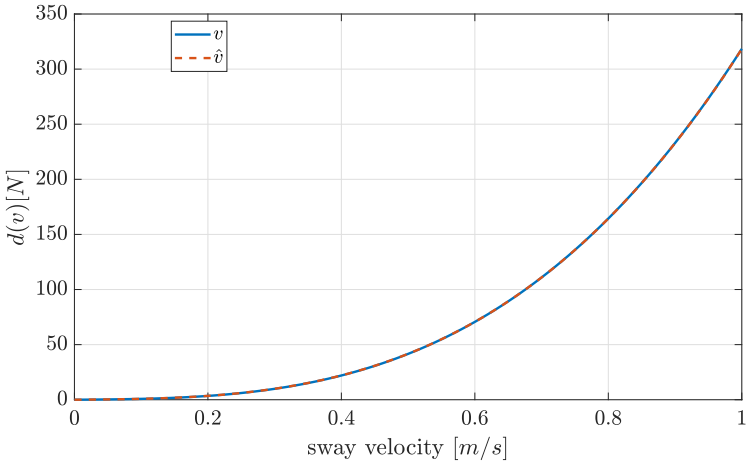

Figure 3.5: Sway damping of grey box model compared to estimated sway damping

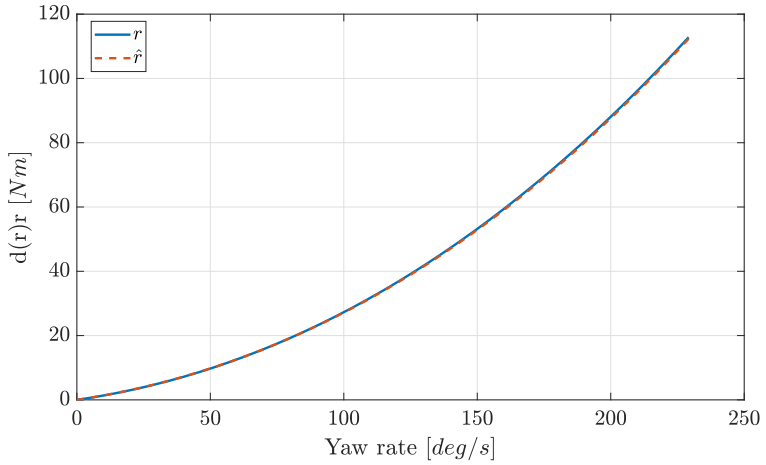

Figure 3.6: Yaw damping of grey box model compared to estimated yaw damping

Since the damping parameters of the grey box model are known, they are compared to the estimated values found from regression, this can be seen in figures 3.4 - 3.6. The identification method is reproducing the damping parameters with great accuracy as the estimated follows the actual damping well. Keep in mind that this is a relatively simplified model with ideal actuator dynamics and a structure that connects to the predicted model very well and therefore these results where expected. The estimated damping parameters can be found in Table 3.1.

3.1.2 Transient

From the step responses as shown in figures 3.1 - 3.3 the transient data from five transient is extracted into set $\mathcal{D}_t = \{(\boldsymbol{\nu}_{t\,1}, \boldsymbol{\nu}_{t\,2}, ...\boldsymbol{\nu}_{t\,N}), (\boldsymbol{\tau}_{t\,1}, \boldsymbol{\tau}_{t2}, ..., \boldsymbol{\tau}_{t\,N})\}$. By applying the simulation based identification method inertia parameters in $\boldsymbol{M}$ are identified.

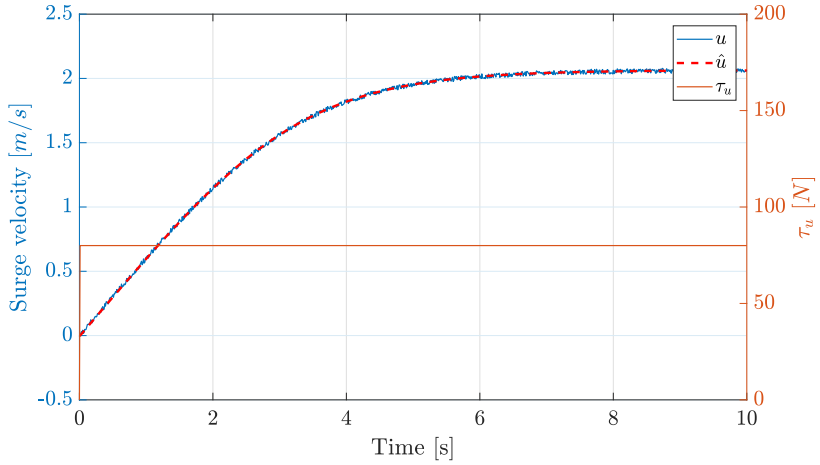

Figure 3.7: Estimated $\hat{u}$ compared to simulated u after m_{11} has been identified. Input force at $80N$.

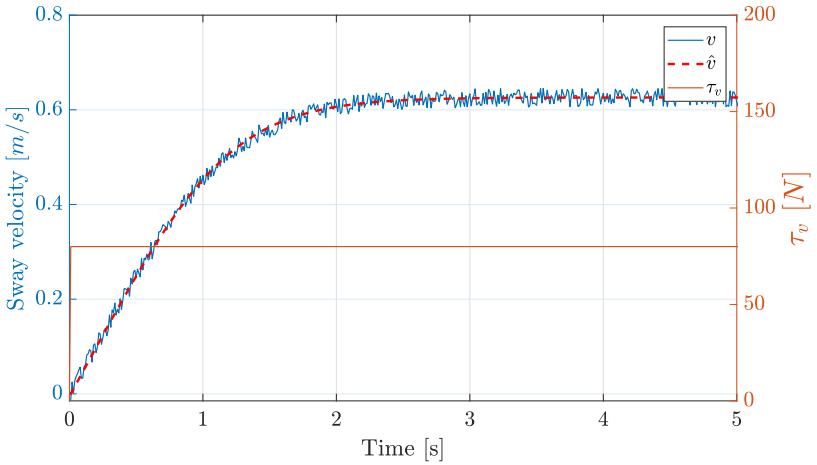

Figure 3.8: Estimated $\hat{v}$ compared to simulated v after m_{22} has been identified. Input force at $80N$.

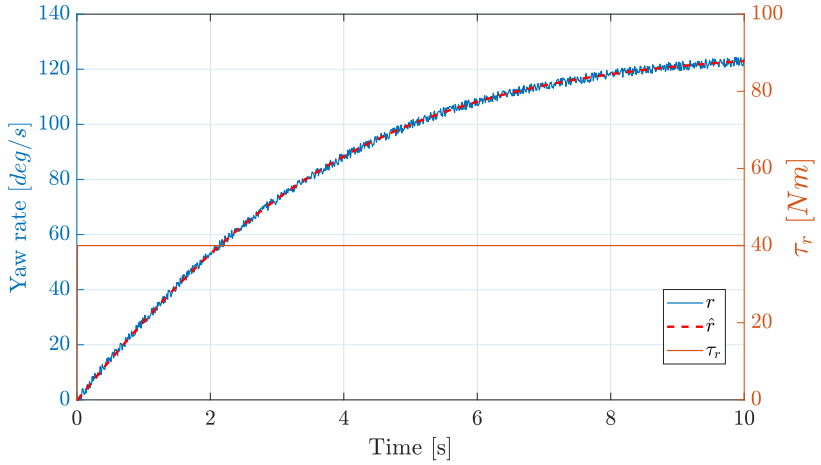

Figure 3.9: Estimated $\hat{r}$ compared to simulated r after m_{33} has been identified. Input force at $40Nm$.

By comparing the velocities in $\mathcal{D}_t$ and the velocities estimated from (2.12) the accuracy of the method can be verified. In the figures 3.7 - 3.9 one of five transient identification performed in each DOF is visualized. It can be seen that the estimated velocity fits well to the simulated after inertia identification. The inertia parameters can be found in table 3.1.

Parameters	Original Value	Estimated Value
m_{11}	131.182	130.5948
m_{22}	156.810	155.053
m_{33}	75.967	75.728
X_u	−2.262	−2.313
$X_{\|u\|u}$	0.000	0.000
X_{uuu}	−8.557	−8.561
Y_v	−4.673	−4.701
$Y_{\|v\|v}$	−0.398	−0.2874
Y_{vvv}	−313.300	−313.523
N_r	−6.916	−6.848
$N_{\|r\|r}$	−4.734	−4.725
N_{rrr}	−0.147	−0.1451

Table 3.1: Grey box model parameter values and estimated parameter values.

3.2 milliAmpere

Two experiments are performed on milliAmpere, these can be found in Appendix A and Appendix B. Due to a recent change of propellers on the thrusters a bollard pull test is completed to map the thruster force. The resulting function can be seen in Figure 3.11. The bollard pull test is found in Appendix A. It should also be mentioned that it was two people onboard during the experiments, which gives some additional weight. The first experiment struggled to give steady state measurements for surge and sway motion as the vessel tend to slip of in coupled motion. Also the size of the test area was to small to perform all the steps continuously. Therefore a second experiment was design to improve the steady state measurements. In the second experiment all steps are started from zero speed. A total of four step responses for surge and sway, and five in yaw are used in the identification process for milliAmpere. The data for surge and sway is gathered from experiment two and the data for yaw is gathered from experiment one. The test conditions for experiment one was -2° Celsius and "Light breeze" according to Beaufort Scale. For experiment two the conditions was -5° Celsius and "Light

Air".

Figure 3.10: The milliAmpere at the day it was christened, June 18. 2018. Picture from https://www.ntnu.no/eit/ttk4851 Photo: Kai T. Dragland/NTNU

milliAmpere	
Length	$5m$
Width	$2.8m$
Propulsion	$2 \times 2kW$ Azimuth Thrusters
Battery	$6 \times 2.4kWh$
Positioning	VECTOR VS330, GNSS and RTK
Sensors	Xsens MTi-10 IMU, Radar, LIDAR, infrared camera.

Table 3.2: milliAmpere spesifications.

3.2.1 Vessel Platform & Hardware

milliAmpere is 5 meters long and 2.8 meters wide and has a rectangular shaped symetric hull design. It is propelled by two azimuth thrusters located at the centerline fore and aft of the vessel, 1.8m from CO. The vessel is fully electric and has a battery bank at 14.4 kWh. Velocities used in the identification part, as plotted in figures 3.12-3.14, are raw data gathered from the navigational unit VECTOR VS330, see Table 3.2.

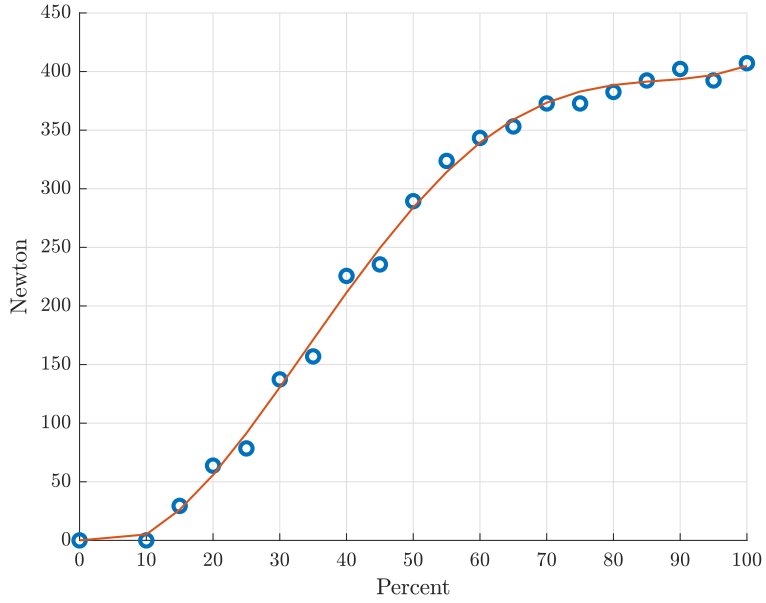

Figure 3.11: Resulting function from bollard pull test. Force from one thruster.

3.3 Results

Figures 3.12 - 3.14 shows the raw data from one of the step responses performed in each DOF.

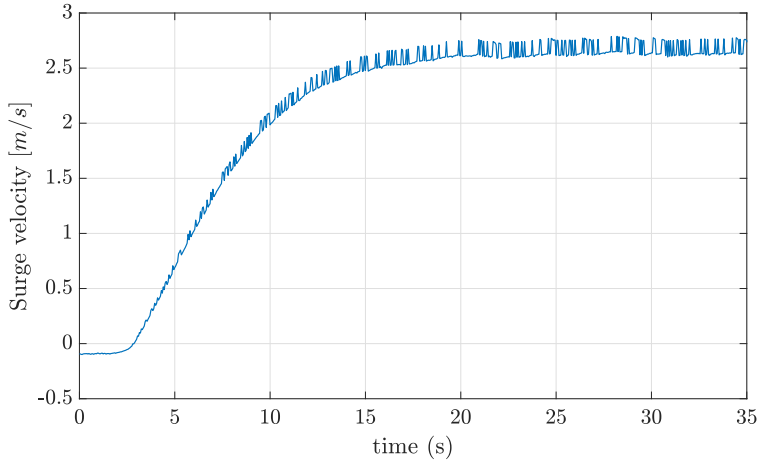

Figure 3.12: Measured surge velocity. Total input force in surge at 809.54 N

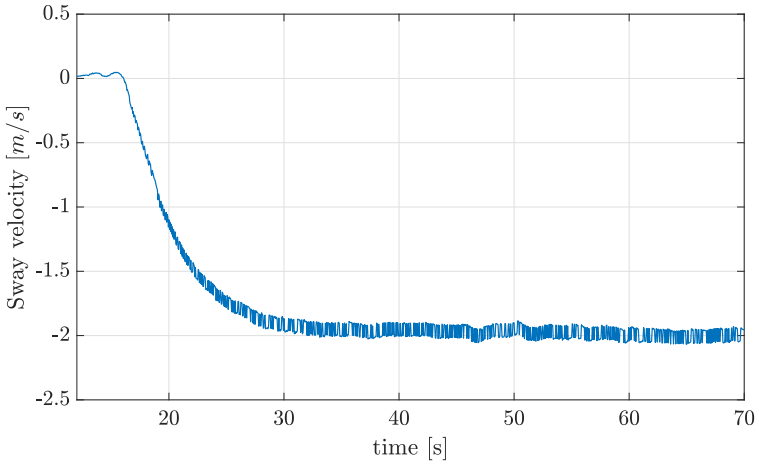

Figure 3.13: Measured sway velocity. Total input force in sway at 809.54 N

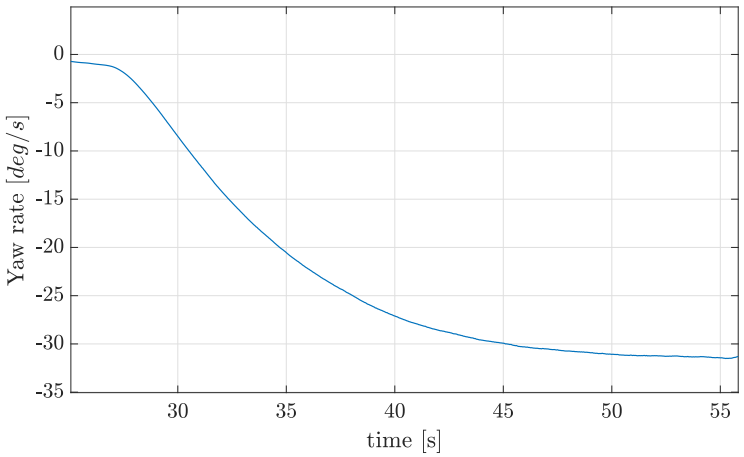

Figure 3.14: Measured yaw rate. Total input force in yaw at 200.8 Nm

3.3.1 Steady State

Steady state data is gathered from the step responses and extracted into $\mathcal{D}_s = \{(\boldsymbol{\nu}_{s1}, \boldsymbol{\nu}_{s2}, ...\boldsymbol{\nu}_{sN}), (\boldsymbol{\tau}_1, \boldsymbol{\tau}_2, ..., \boldsymbol{\tau}_N)\}$. By minimizing (3.3) where λ is found by CV, using nonlinear optimization, a solution is found.

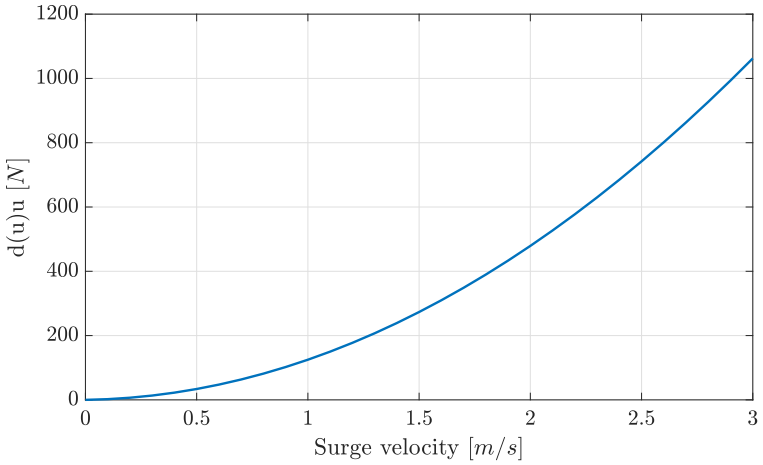

Figure 3.15: Surge damping of milliAmpere

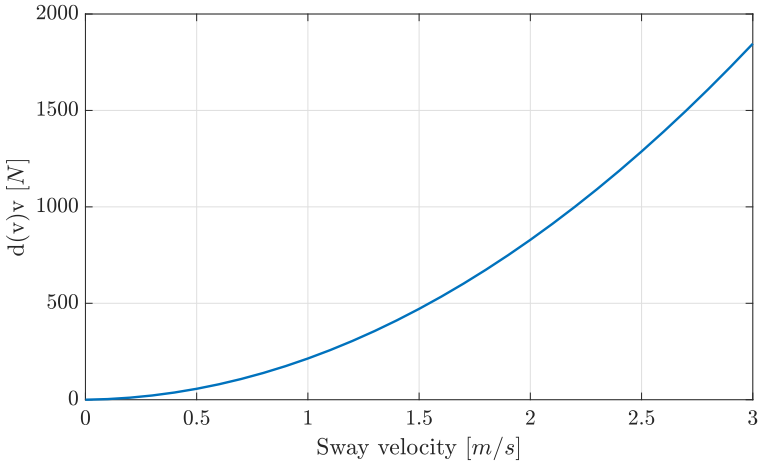

Figure 3.16: Sway damping of milliAmpere

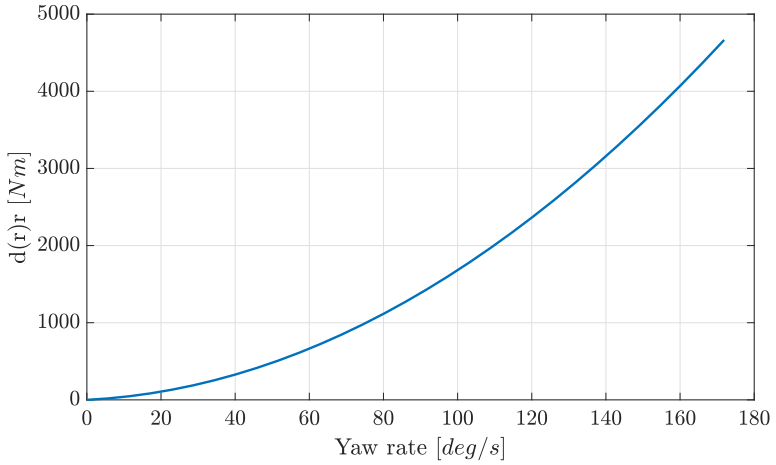

Figure 3.17: Yaw damping of milliAmpere

The results from the identification of damping parameters can be viewed in table 3.4. The figures 3.15 - 3.17 shows the damping for milliAmpere in surge, sway and yaw. It can be seen that surge has the lowest damping force and sway the highest. This is expected and can be explained by the drag force caused by the vessel pushing through the water. Due to hull design, a larger area is forced through the water when the vessel performs yaw and sway motion than in surge. Also it is noticeable that the third order damping parameters for surge, sway and yaw are zero. The milliAmpere has a top speed of $2.6\frac{m}{s}$, which is relative slow, thus the damping force is explained well by the sum of linear and quadratic damping terms. This implies that it would be sufficient with quadratic damping terms in $\boldsymbol{D}(\boldsymbol{\nu})$.

3.3.2 Transient

From step responses the transient data is extraced into set $\mathcal{D}_t = \{(\boldsymbol{\nu}_{t\,1}, \boldsymbol{\nu}_{t\,2}, ...\boldsymbol{\nu}_{t\,N}), (\boldsymbol{\tau}_{t\,1}, \boldsymbol{\tau}_{t2}, ..., \boldsymbol{\tau}_{t\,N})\}$. By applying the simulation based identification method, inertia parameters in $\boldsymbol{M}$ are identified. For surge and sway velocity, a total of four transients are obtained, and for yaw rate a total of five transients. The corresponding input force and moment for those transients can be found in Table 3.3.

Transient	Input force Surge	Input force Sway	Input moment yaw
1	$111.6N$	$111.6N$	$200.8Nm$
2	$678,8N$	$678,8N$	$760.9Nm$
3	$777.0N$	$777.0N$	$1221.8Nm$
4	$809.5N$	$809.5N$	$1398.6Nm$
5	-	-	$1457.2Nm$

Table 3.3: Transients and input force/moment

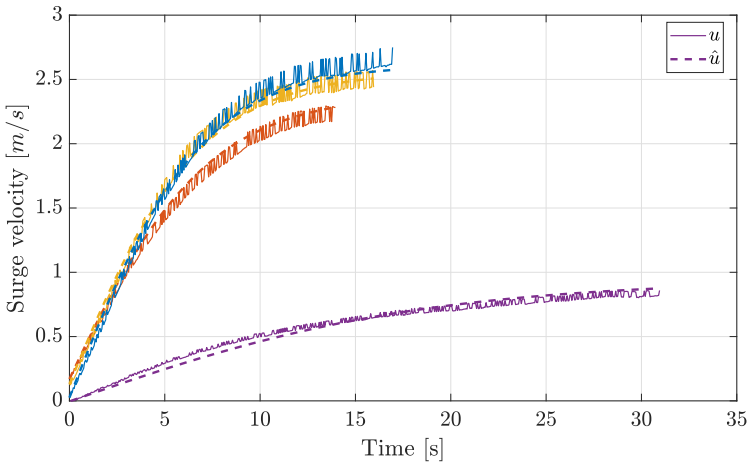

Figure 3.18: Comparison of real u and estimated $\hat{u}$, for four transients, with $m_{11} = 2137Kg$.

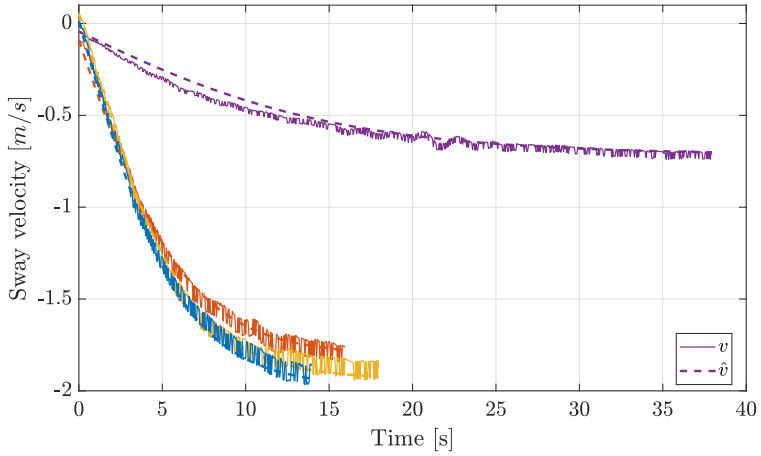

Figure 3.19: Comparison of real v and estimated $\hat{v}$, for four transients, with $m_{22} = 2528Kg$.

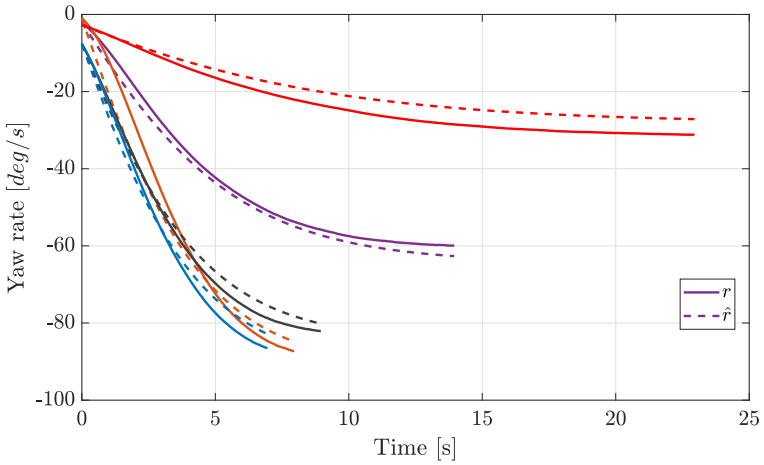

Figure 3.20: Comparison of real r and estimated $\hat{r}$, for five transients, with $m_{33} = 3942Kgm^2$.

The result from the identification of inertia parameters can be viewed in Table 3.4. Figures 3.18 through 3.20 shows how the estimated velocity fits the real velocity after identification of the inertia parameters. As expected the three parameters in $\boldsymbol{M}$ are different. Due to the hull design of milliAmpere, sway motion will move more water than surge motion, hence m_{22} is larger than m_{11}. The values also correspond well to the size of the vessel.

Parameters	**Value**	**Unit**
m_{11}	2137.734	kg
m_{22}	2528.350	kg
m_{33}	3942.080	kgm^2
X_u	-10.342	$\frac{kg}{s}$
$X_{\|u\|u}$	-114.581	$\frac{kg}{s}$
X_{uuu}	0	$\frac{kg}{s}$
Y_v	-13.011	$\frac{kg}{s}$
$Y_{\|v\|v}$	-200.748	$\frac{kg}{s}$
Y_{vvv}	0	$\frac{kg}{s}$
N_r	-201.022	$\frac{kg}{s}$
$N_{\|r\|r}$	-424.081	$\frac{kg}{s}$
N_{rrr}	0	$\frac{kg}{s}$

Table 3.4: Estimated damping and inertia parameters for milliAmpere.

Chapter 4

Conclusions

In this project a 3-DOF nonlinear model (2.3) is proposed as a candidate to describe the dynamics of the milliAmpere ferry. By designing and performing two experiments, raw data for uncoupled motion in 3-DOF is gathered. The raw data is then separated and used in a steady state and transient analysis. Also as it is necessary to know the exact force coming from the two thrusters, a bollard pull test is completed and a mapping between input signal and output force is created. Two different methods are used to identify the unknown parameters in (2.3) and verified by testing it on a grey box model. To identify the damping matrix, linear regression is used and for identification of the inertia matrix, a simulation based identification method is performed.

The results from the grey box model experiment shows that the methods are able to predict accurate estimations for both damping and inertia parameters. By using the original values for the grey box as a reference it can be seen in Table 3.1 that both methods are able to reproduce the parameters with relative small error. As for the experiments on milliAmpere, the resulting parameter values can be viewed in Table 3.4. With uncoupled steady state analysis and linear regression the damping matrix $\boldsymbol{D}(\boldsymbol{\nu})$ is found to be explained well by the sum of linear and quadratic terms in surge, sway and yaw. The inertia parameters are identified by a simulation based method and the resulting values are reasonable. Both identification methods are able to reproduce parameters with small error and together they are able to identify dynamic systems.

4.1 Future Work

- Use these methods to identify parameters of a coupled model.
- Use the model for model based control and verify performance by experiments.

Appendix A

Test Plan 1

Model Identification Experiments on milliAmpere
Test Plan 1

Anders Aglen Pedersen

November 2018

Safety

When operating the vessel at sea it must always be two persons on board. The location of the safety equipment and a plan for act due to unsuspected events like loss of propulsion, system failure, power loss, fire etc. must be undergone for all operators.

Test Goal

The main goal for this experiment is to gather transient and steady state data for surge, sway and yaw motion with the associated input force. This will be used for identification of parameters in mathematical model.

1 Test Platform

Due to recent change of propellers on the vessel a Bollard pull test must be completed before the identification experiments starts, this is to ensure that the input force of the thrusters is known. The vessel has two thrusters than can rotate 360 degrees, $[-180°, 180°]$ where $0°$ is in surge. The control system will be used to manually control the desired thruster force and angles. The system runs Robotic Operating System ROS which has implemented a tool called rosbag that is an unified console tool for recording data, playback data, and other operations. This will be used to log the measurements.

2 Bollard Pull Test

The Bollard pull test will result in a function, which gives the output force in Newton. Assuming that both thrusters are identical we have that $\boldsymbol{\tau} = f(u_m)$, where u_m is motor speed [-100%,100%] and $\boldsymbol{\tau}$ is thruster force [N].

A rope is fastened to a bollard on the quay and two attachment points on the vessel. Between the bollard and the vessel is a weight used to measure the force from the thrusters. It is important that the bollard and the attachment points on the vessel are aligned. The motor speed will be controlled manually through ROS.

2.1 Safety cautions for Bollard pull test

- Control the ropes for damages
- All persons on board the vessel must be seated during the test.

- Make sure that other vessels, paddlers, swimmers etc. are at a safe distance during the test.
- Make sure all attachment points are properly done.

2.2 Test

1. Start with Front thruster and set motor speed according to row 1 in table 1 and write down the measured force.
2. Proceed to next row in table 1 and write down measured force.
3. Repeat step 2 until 100%.

Motor speed [%]	Front thruster [N]	Front thruster reversed [N]
10		
15		
20		
25		
30		
35		
40		
45		
50		
55		
60		
65		
70		
75		
80		
85		
90		
95		
100		

Table 1: Bollard pull test table.

3 Identification Experiment

The actuator space can be mapped in

$$\boldsymbol{\mathcal{A}} = \{\boldsymbol{\alpha} \in \mathbb{S}^2 | -180^\circ \leq \alpha \leq 180^\circ\}$$

and

$$\boldsymbol{\mathcal{F}} = \{\boldsymbol{f} \in \mathbb{R}^2 | 0 \leq f \leq 100\%\}$$

where $\boldsymbol{f}$ is thruster force in percent and $\boldsymbol{\alpha}$ is thruster angle. The angles $\boldsymbol{\alpha}$ is fixed for each of the three DOF, that is $\boldsymbol{\alpha} = [0, 0]^T$ for steps in surge, $[90^\circ, 90^\circ]^T$ for steps in sway and $[90^\circ, -90^\circ]^T$ for steps in yaw. A series of step responses is performed in each DOF and it is crucial for the vessel to achieve steady state motion between the steps.

Commanded steps for [0-100%] are $\boldsymbol{f_{inc}} \in \{(0, 0), (20, 20), (40, 40), ..., (100, 100)\}\%$.
Commanded steps for [100-0%] are $\boldsymbol{f_{dec}} \in \{(100, 100), (80, 80), (60, 60), ..., (0, 0)\}\%$.

The experiment will be performed in this order:

- Steps in surge, $[0, 100\%]$ with increment of 20% for each step.
- Steps in surge, $[100\%, 0]$ with decrement of 20% for each step.
- Steps in sway, $[0, 100\%]$ with increment of 20% for each step.
- Steps in sway, $[100\%, 0]$ with decrement of 20% for each step.
- Steps in yaw, $[0, 100\%]$ with increment of 20% for each step.
- Steps in yaw, $[100\%, 0]$ with decrement of 20% for each step.

3.1 Experiment 1

Make sure that the logging is started and a new rosbag is created. Write down the time from the system clock.

3.1.1 Surge test

1. Start at $\boldsymbol{\nu} = 0$ and use $\boldsymbol{\alpha} = [0, 0]^T$ for thruster angles.
2. Start the step serie according to $\boldsymbol{f_{inc}}$ and let the vessel reach steady state motion for 5 seconds before initiating next command in $\boldsymbol{f_{inc}}$ until 100%.
3. Start the step serie according to $\boldsymbol{f_{dec}}$ and let the vessel reach steady state motion for 5 seconds before initiating next command in $\boldsymbol{f_{dec}}$ until 0%.
4. Set thrust force to zero and let the vessel come to full stop.

3.1.2 Sway test

1. Start at $\boldsymbol{\nu} = 0$ and use $\boldsymbol{\alpha} = [90^\circ, 90^\circ]^T$ for thruster angles.
2. Start the step serie according to $\boldsymbol{f_{inc}}$ and let the vessel reach steady state motion for 5 seconds before initiating next command in $\boldsymbol{f_{inc}}$ until 100%.
3. Start the step serie according to $\boldsymbol{f_{dec}}$ and let the vessel reach steady state motion for 5 seconds before initiating next command in $\boldsymbol{f_{dec}}$ until 0%.
4. Set thrust force to zero and let the vessel come to full stop.

3.1.3 Yaw test

1. Start at $\boldsymbol{\nu} = 0$ and use $\boldsymbol{\alpha} = [90°, -90°]^T$ for thruster angles.
2. Start the step serie according to $\boldsymbol{f_{inc}}$ and let the vessel reach steady state motion for 5 seconds before initiating next command in $\boldsymbol{f_{inc}}$ until 100%.
3. Start the step serie according to $\boldsymbol{f_{dec}}$ and let the vessel reach steady state motion for 5 seconds before initiating next command in $\boldsymbol{f_{dec}}$ until 0%.
4. Set thrust force to zero and let the vessel come to full stop.

Appendix B

Test Plan 2

Model Identification Experiments on milliAmpere
Test Plan 2

Anders Aglen Pedersen

December 2018

Safety

When operating the vessel at sea it must always be two persons on board. The location of the safety equipment and a plan for act due to unsuspected events like loss of propulsion, system failure, power loss, fire etc. must be undergone for all operators.

Test goal

The main goal for this experiment is to gather transient and steady state data for surge and sway motion.

1 Test platform

The control system on board will be used for logging the desired input force and output velocities. The vessel has two thrusters than can rotate 360 degrees, $[-180°, 180°]$ where $0°$ is in surge. The control system will be used to manually control the desired thruster force and angles. The system runs ROS which has implemented a tool called rosbag that is an unified console tool for recording data, playback data, and other operations. This will be used for logging data.

2 Identification experiment 2

The actuator space can be mapped in

$$\boldsymbol{\mathcal{A}} = \{\boldsymbol{\alpha} \in \mathbb{S}^2 | -180° \leq \alpha \leq 180°\}$$

and

$$\boldsymbol{\mathcal{F}} = \{\boldsymbol{f} \in \mathbb{R}^2 | 0 \leq f \leq 100\%\}$$

where $\boldsymbol{f}$ is thruster force in percent and $\boldsymbol{\alpha}$ is thruster angle. The angles $\boldsymbol{\alpha}$ is fixed for each of the three DOF, that is $\boldsymbol{\alpha} = [0, 0]^T$ for steps in surge and $[90°, 90°]^T$ for steps in sway. Five step responses is performed in surge and sway and it is crucial for the vessel to achieve steady state motion between the steps.

Commanded steps for [0-100%] are $\boldsymbol{f} \in \{(20, 20), (40, 40), ..., (100, 100)\}\%$.

The experiment will be performed in this order:

- Steps in surge, $[0, 100\%]$
- Steps in sway, $[0, 100\%]$

2.1 Experiment

Make sure that a new rosbag is created and logging is started. Write down the time from the system clock.

2.1.1 Surge test

1. Start at $\boldsymbol{\nu} = 0$ and use $\boldsymbol{\alpha} = [0, 0]^T$ for thruster angles.
2. Start the step serie according to $\boldsymbol{f}$ and let the vessel reach steady state motion for 5 seconds
3. Set thrust force to zero and let the vessel come to full stop.
4. Initiate next command in $\boldsymbol{f}$ and let the vessel reach steady state motion for 5 seconds.
5. Repeat 3 and 4 until 100%.

2.1.2 Sway test

1. Start at $\boldsymbol{\nu} = 0$ and use $\boldsymbol{\alpha} = [90, 90]^T$ for thruster angles.
2. Start the step serie according to $\boldsymbol{f}$ and let the vessel reach steady state motion for 5 seconds
3. Set thrust force to zero and let the vessel come to full stop.
4. Initiate next command in $\boldsymbol{f}$ and let the vessel reach steady state motion for 5 seconds.
5. Repeat 3 and 4 until 100%.

References

Bishop, C. M. (2006). *Pattern Recognition and Machine Learning*, Springer.

Bitar, G. I. (2018). Report on performing system identification using simulation as a predictor. Unpublished report by Bitar, Glenn. I. Department of Engineering Cybernetics, NTNU.

Eriksen, B.-O. H. and Breivik, M. (2017). Modeling, identification and control of high-speed ASVs: Theory and experiments, *Sensing and Control for Autonomus Vehicles*, Springer, chapter 5, pp. 407 – 431.

Faltinsen, O. M. (2005). *Hydrodynamics of High-Speed Marine Vehicles*, Cambridge University Press.

Fossen, T. I. (2011). *Handbook of Marine Craft Hydrodynamics and Motion Control*, John Wiley & Sons, Ltd.

Hastie, Trevor. Tibshirani, R. F. J. (2009). *The Elements of Statistical Learning*, Springer.

Jeffrey C. Lagarias, James A. Reeds, M. H. W. and Wright, P. E. (1998). Convergence properties of the nelder-mead simplex method in low dimensions, *SIAM Journal of Optimization* **9**(1): 112 – 147.

Kongsberg (2018). Autonomous ship project, key facts about yara birkeland.
URL: *https://www.km.kongsberg.com/ks/web/nokbg0240.nsf/AllWeb/4B8113B707A50A4FC125811D00407045*

Lyngstadaas, O. N., Saeterdal, T. E., Sorensen, M. E. N. and Breivik, M. (2018). Improvement of ship motion control using a magnitude-rate saturation model, *2018 IEEE Conference on Control Technology and Applications (CCTA)*, IEEE.
URL: *https://doi.org/10.1109/ccta.2018.8511451*

Nocedal, J. and Wright, S. J. (2006). *Numerical Optimization*, second edn, Springer.

Rolls-Royce (2018). Rolls-royce and finferries demonstrate world's first fully autonomous ferry.
URL: *https://www.rolls-royce.com/media/press-releases/2018/03-12-2018-rr-and-finferries-demonstrate-worlds-first-fully-autonomous-ferry.aspx*

Sonneburg, C. R. and Woolsey, C. A. (2013). Modeling, identification, and control of an unmanned surface vehicle, *Journal of Field Robotics* **30**(3): 371 – 398.

Teknisk-Ukeblad (2018). Her demonstrerer de selvkjørende milliampere.
URL: *https://www.tu.no/artikler/her-demonstrerer-de-selvkjorende-milliampere-na-skal-de-bygge-ferge-pa-12-meter/447398*